

Neutron skin thickness of ^{208}Pb , $^{116,120,124}\text{Sn}$, and ^{40}Ca determined from reaction cross sections of ^4He scattering

Masayuki Matsuzaki

Department of Physics, Fukuoka University of Education, Munakata, Fukuoka 811-4192, Japan

Shingo Tagami

Department of Physics, Kyushu University, Fukuoka 819-0395, Japan

Masanobu Yahiro*

Department of Physics, Kyushu University, Fukuoka 819-0395, Japan

(Dated: December 23, 2021)

Background: We constructed the Kyushu chiral g -matrix and confirmed its reliability at $30 \lesssim E_{\text{in}} \lesssim 100$ MeV and $250 \lesssim E_{\text{in}} \lesssim 400$ MeV for ^{12}C scattering. Reaction cross section data of ^4He scattering are available for some nuclides including ^{208}Pb . PREX II collaboration reported a thick neutron skin for ^{208}Pb .

Purpose: Our purpose is to deduce neutron skin thicknesses of ^{208}Pb and some other nuclides from reaction cross sections calculated in terms of the double folding model with the g -matrix.

Methods: We fold the g -matrix and densities given by mean field calculations. In order to remedy less-constrainedness of the neutron sector, we renormalize densities so as to reproduce the observed cross sections.

Results: We found that a 3.4 % renormalization is necessary for ^{208}Pb . The neutron density obtained from renormalization results in $R_{\text{skin}} = 0.416 \pm 0.146$ fm by confronting the precision proton radius.

Conclusions: Our result is consistent with PREX II and therefore supports larger slope parameter L . Results for ^{40}Ca and ^{124}Sn are also consistent with R_{skin} deduced from other experiments. For $^{116,120}\text{Sn}$ the present method gives thicker skins.

I. INTRODUCTION

In heavy atomic nuclei, neutrons outnumber protons as the mass number increases so as to mitigate the Coulomb repulsion between protons. This leads to the difference in the spatial distribution — the neutron skin emerges, where the skin thickness is defined as the difference in the root mean square radii between neutrons and protons. This isovector property is not only one of the basic quantities in the structure of finite, terrestrial nuclei but determines the equation of state (EoS) of infinite nuclear matter in astrophysical objects such as neutron stars and exploding supernovae.

Information about nuclear radii is extracted from various experimental means. In contrast, theoretically, only mean-field calculations are available for heavy nuclei practically. Energy density functionals adopted in mean-field calculations contain many parameters of which numerical values are informed by basic observables such as binding energies, radii and so on, of representative stable and some unstable nuclides. The mean-field calculations predict various quantities including nuclear radii of other nuclides. Precision of proton radii among them is thought to be high because of cleanness of electron scatterings that inform the parameters of the proton sector. In contrast, neutron radii and accordingly skin thicknesses are less determined. This suggests that the calculated values of neutron radii should be critically assessed. In other words, it would be better to be based more directly on experimental information. One of such directions is to determine nuclear matter radius from reaction cross sections σ_{R} of

nucleon-nucleus and/or nucleus-nucleus scatterings and then deduce neutron radius, and consequently skin thickness, by confronting the precision proton radius obtained by electron scatterings.

As proposed by Horowitz et al. [1], on the other hand, parity-violating electron scatterings using polarized beams give directly neutron radii. By confronting them with the proton radii, skin thickness can be obtained. Actually, the PREX II experiment reported a precision datum of the neutron skin thickness of ^{208}Pb [2]; namely,

$$R_{\text{skin}}^{208}(\text{PREX II}) = 0.283 \pm 0.071 \text{ fm}. \quad (1)$$

The $R_{\text{skin}}^{208}(\text{PREX II})$ gives larger the slope parameter L and supports stiffer EoSs. As a famous EoS, we can consider APR [3]. It yields $R_{\text{skin}}^{208} = 0.16$ fm. This value is out of $R_{\text{skin}}^{208}(\text{PREX II})$. This is an interesting issue to be solved, since this calculation is believed to be best for symmetric and neutron matter. As for the density dependence of the symmetry energy, studied with heavy-ion collisions, collective excitation in nuclei (especially Pygmy Dipole Resonances) and neutron-star calculations, a good brief review is shown in Ref. [4].

In relation to the present subject, our group has been studying nuclear reaction observables, including σ_{R} relevant to the present purpose, in terms of a microscopic optical potential based on a chiral g -matrix [5]. This g -matrix was constructed by Kohno [6] by taking into account the next-to-next-to-next-to leading order (N^3LO) two-body force and the NNLO three-body force in chiral perturbation. Toyokawa et al. localized the non-local g -matrix, and we call it the Kyushu chiral g -matrix [5]. Its numerical values for selected discrete energies are presented in a web page for public use [7]. In that work,

* orion093g@gmail.com

σ_R of ${}^4\text{He} + {}^{58}\text{Ni}$ and ${}^4\text{He} + {}^{208}\text{Pb}$ were studied paying attention to the effect of the three-body force, in terms of the double-folding model (DFM) adopting a microscopic density of the Gogny-D1S Hartree-Fock (HF) for the targets and a phenomenological one [8] for the projectile.

In Ref. [9], we first predicted the ground-state properties, such as binding energies, one- and two-neutron separation energies and various radii, of Ca isotopes adopting Gogny-D1S Hartree-Fock-Boboliubov (HFB) with and without the angular-momentum projection (AMP). Using the nuclear densities given by this structure calculation and the Kyushu chiral g -matrix, we predicted σ_R for scattering of Ca isotopes on a ${}^{12}\text{C}$ target with DFM, after confirming its reliability at each incident energy for ${}^{12}\text{C} + {}^9\text{Be}$, ${}^{12}\text{C}$, and ${}^{27}\text{Al}$ scatterings.

After the PREX II result [2] is announced, we performed a single-folding model calculation of σ_R of $p + {}^{208}\text{Pb}$ scattering by adopting the Kyushu chiral g -matrix [10] and the Gogny-HFB. The important finding of this study is that the calculated σ_R are 3 % smaller than the experimental values in the energy range in which the reliability of the Kyushu chiral g -matrix has been confirmed and the Gogny HFB reproduces the observed proton radii well. Then we assume that this originates from the less-confirmed mean-field parameters for the neutron sector and we attempted to renormalize the HFB+AMP neutron density to reproduce the σ_R data. The neutron radius deduced from the energy-averaged σ_R through the matter radius leads to a neutron skin thickness that agrees with the PREX II result well.

The purpose of the present work is to examine further the present method — extract the neutron radius from σ_R given by the Kyushu chiral g -matrix and the phenomenologically renormalized mean-field density — by revisiting the ${}^4\text{He} + {}^{208}\text{Pb}$ scattering studied in Ref. [5] and comparing with the $p + {}^{208}\text{Pb}$ result of Ref. [10]. Then we study some lighter nuclides.

II. MODEL

The model adopted in this work is essentially the same as that in Ref. [10], aside from the optical potential is obtained by double folding for ${}^4\text{He} + {}^{208}\text{Pb}$, rather than single folding for $p + {}^{208}\text{Pb}$. The double folding is performed for the Kyushu chiral g -matrix and the adopted nuclear densities.

As the densities of ${}^{208}\text{Pb}$ we newly examined the Skyrme HFB [11] with the SLy7 parameter set, which is an improved version of the widely used SLy4 [12], in addition to the D1S-GHFB+AMP ones [9]. As for ${}^4\text{He}$, again we use the phenomenological density [8].

The potential U consists of the direct part (U^{DR}) and the exchange part (U^{EX}):

$$U^{\text{DR}}(\mathbf{R}) = \sum_{\mu,\nu} \int \rho_{\text{P}}^{\mu}(\mathbf{r}_{\text{P}}) \rho_{\text{T}}^{\nu}(\mathbf{r}_{\text{T}}) g_{\mu\nu}^{\text{DR}}(s; \rho_{\mu\nu}) d\mathbf{r}_{\text{P}} d\mathbf{r}_{\text{T}}, \quad (2)$$

$$U^{\text{EX}}(\mathbf{R}) = \sum_{\mu,\nu} \int \rho_{\text{P}}^{\mu}(\mathbf{r}_{\text{P}}, \mathbf{r}_{\text{P}} - \mathbf{s}) \rho_{\text{T}}^{\nu}(\mathbf{r}_{\text{T}}, \mathbf{r}_{\text{T}} + \mathbf{s}) \times g_{\mu\nu}^{\text{EX}}(s; \rho_{\mu\nu}) \exp[-i\mathbf{K}(\mathbf{R}) \cdot \mathbf{s}/M] d\mathbf{r}_{\text{P}} d\mathbf{r}_{\text{T}}, \quad (3)$$

where $\mathbf{s} = \mathbf{r}_{\text{P}} - \mathbf{r}_{\text{T}} + \mathbf{R}$ for the coordinate \mathbf{R} between the projectile (P) and target (T). The coordinate \mathbf{r}_{P} (\mathbf{r}_{T}) denotes the location for the interacting nucleon measured from the center-of-mass of P (T). Each of μ and ν stands for the z -component of isospin; $1/2$ means neutron and $-1/2$ does proton. The original form of U^{EX} is a non-local function of \mathbf{R} , but it has been localized in Eq. (3) with the local semi-classical approximation in which P is assumed to propagate as a plane wave with the local momentum $\hbar\mathbf{K}(\mathbf{R})$ within a short range of the nucleon-nucleon interaction, where $M = AA_{\text{T}}/(A + A_{\text{T}})$ for the mass number A (A_{T}) of P (T). The validity of this localization is shown in Ref. [13].

The direct and exchange parts, $g_{\mu\nu}^{\text{DR}}$ and $g_{\mu\nu}^{\text{EX}}$, of the effective nucleon-nucleon interaction (g -matrix) depend on the local density

$$\rho_{\mu\nu} = \sigma^{\mu} \rho_{\text{T}}^{\nu}(\mathbf{r}_{\text{T}} + \mathbf{s}/2) \quad (4)$$

at the midpoint of the interacting nucleon pair, where σ^{μ} is the Pauli matrix of a nucleon in P. This choice of the local density is quite successful for ${}^4\text{He}$ scattering, as shown in Ref. [14].

The renormalization, that is, the scaling of the density $\rho(\mathbf{r})$, will be performed as follows: We can obtain the scaled density $\rho_{\text{scaling}}(\mathbf{r})$ from the original density $\rho(\mathbf{r})$ as

$$\rho_{\text{scaling}}(\mathbf{r}) = \frac{1}{\alpha^3} \rho(\mathbf{r}/\alpha) \quad (5)$$

with a scaling factor

$$\alpha = \sqrt{\frac{\langle \mathbf{r}^2 \rangle_{\text{scaling}}}{\langle \mathbf{r}^2 \rangle}}. \quad (6)$$

The actual procedure to determine α (of p and n) for each case is: Firstly we scale the proton density so as to be $R_{\text{p}}(\text{scaling}) = R_{\text{p}}(\text{exp})$ although is a tiny adjustment, secondly we scale the neutron density so as that the σ_R reproduces the data in average with respect to E_{in} .

III. RESULTS AND DISCUSSION

A. ${}^{208}\text{Pb}$

As a preparation, first we compare two sets of calculated densities in Fig. 1. The two sets practically coincide in the sense that the effect of the slight difference in the deep inside on σ_R is negligible and the differences in the calculated radii (column 1 and 2 in Table I) are less than 1 %.

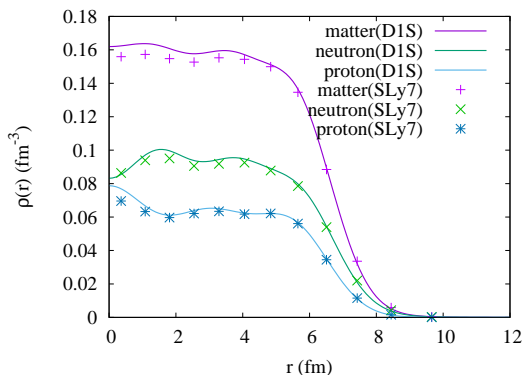


FIG. 1. r dependence of densities, $\rho_p(r)$, $\rho_n(r)$, $\rho_m(r)$, for ^{208}Pb calculated with D1S-GHFB+AMP and SLy7-HFB. Dashed curves from the bottom to the top denote the $\rho_p(r)$, $\rho_n(r)$, $\rho_m(r)$ of D1S-GHFB, respectively. Symbols correspond to the SLy7-HFB densities.

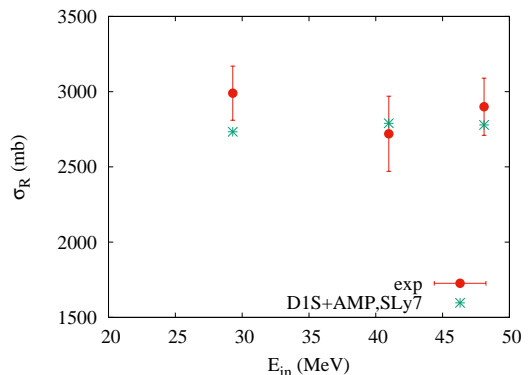


FIG. 2. E_{in} dependence of reaction cross sections σ_R for $^4\text{He} + ^{208}\text{Pb}$ scattering. Note that E_{in} is the incident energy per nucleon. Asterisks stand for the results of D1S-GHFB+AMP and SLy7-HFB. The data are taken from Ref. [16].

TABLE I. Various radii of ^{208}Pb , given in fm. Column 1 and 2 are the results of direct calculations with the Gogny-HFB+AMP and the Skyrme-HFB, respectively. Column 3 is taken from Ref. [2]. Column 4 and 5 are deduced from the renormalized densities for p scattering [10] and ^4He scattering (present work), respectively. $R_p = 5.444$ fm is taken from Ref. [15].

	D1S	SLy7	PREX II	p	^4He
R_n	5.580	5.619		5.722 ± 0.035	5.860 ± 0.146
R_p	5.443	5.469		5.444	5.444
R_{skin}	0.137	0.150	0.283 ± 0.071	0.278 ± 0.035	0.416 ± 0.146
R_m	5.526	5.560		5.614 ± 0.022	5.700 ± 0.146

We present the calculated σ_R in Fig. 2 comparing with the data. Adopting the Kyushu chiral g -matrix folding model, of which reliability in the energy range $29.3 \leq E_{in} \leq 85$ MeV has been confirmed [9], calculated σ_R are 96.6% of the data in average. This is very similar to the p + ^{208}Pb result in Ref. [10], 97% in $30 \leq E_{in} \leq 100$ MeV.

According to this observation, we apply the same renormalization procedure, that is, we scale the D1S-GHFB+AMP densities so as to reproduce σ_R for each E_{in} under the condition that the proton radius given by the scaled density agrees with the data from electron scattering, and take the weighted mean and its error for the resulting R_m . From the resulting $R_m = 5.700 \pm 0.146$ fm and $R_p = 5.444$ fm, we obtain $R_n = 5.860 \pm 0.146$ fm. This leads to $R_{skin} = 0.416 \pm 0.146$ fm that is consistent with the PREX II result as shown in Table I. The present result for $^4\text{He} + ^{208}\text{Pb}$, in addition to that for p + ^{208}Pb in Ref. [10], strongly suggests that the less-determined mean-field parameters in the neutron sector tend to lead to smaller R_n and consequently thin skins at least in heavy nuclei such as ^{208}Pb .

This looks consistent with the result of the dispersive optical model analysis, in which the single-particle selfenergies are informed by various observed quantities, $R_{skin} = 0.25 \pm 0.05$ fm [17]. The remaining unresolved issue is the consistency with the result of the other clean method, the electric dipole polarizability α_D , as explicitly addressed in Ref. [18]; α_D obtained from photoabsorption reactions leads to a thin $R_{skin} = 0.156^{+0.025}_{-0.021}$ fm [19] through the correlation [20].

B. $^{116,120,124}\text{Sn}$

In order to see to what extent the picture presented above holds in lighter nuclides, we study stable Sn isotopes in this subsection. Figure 3 presents the experimental and calculated σ_R for ^{120}Sn . The latter is smaller than the central value of the former although located within the error bar at all three E_{in} . The direct calculation with the SLy7 parameter set gives $R_{skin} = 0.123$ fm as in column 1 in Table II. This is slightly smaller than the HF+BCS result with the SLy4 set reported in Ref. [21]. Column 2 reports the result of the same renormalization procedure as above, adopting $R_p = 4.583$ fm [22]. The resulting skin is too thick.

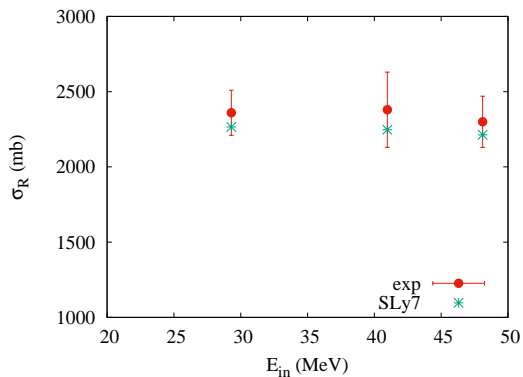


FIG. 3. E_{in} dependence of reaction cross sections σ_R for ${}^4\text{He} + {}^{120}\text{Sn}$ scattering. Asterisks show the results of SLy7-HFB. The data are taken from Ref. [16].

TABLE II. Various radii of ${}^{120}\text{Sn}$, given in fm. Column 1 is the result of the direct calculation with the Skyrme-HFB. Column 2 is that of the same renormalization procedure applied to the data [16] with $R_p = 4.583$ fm, determined from the charge density data [22]. Column 3 and 4 are taken from Refs. [23, 24].

	SLy7	${}^4\text{He}$	Krasznahorkay	Hashimoto
R_n	4.719	4.959 ± 0.140		
R_p	4.595	4.583		
R_{skin}	0.123	0.377 ± 0.140	0.18 ± 0.07	0.148 ± 0.034
R_m	4.668	4.806 ± 0.140		

Then we consult other experimental information obtained by dipole resonances. The first one is given by the spin-dipole resonance excited by the $({}^3\text{He}, t)$ reaction [23]. A model-dependent value $R_{skin} = 0.18 \pm 0.07$ fm is given by normalizing to a theoretical result. The second one is given through the correlation with α_D [20] obtained by the (\vec{p}, \vec{p}') reaction [24]. The authors conclude $R_{skin} = 0.148 \pm 0.034$ fm. These are summarized in Table II. Although the correlation between R_{skin} and α_D is argued not to be consistent with relativistic mean-field calculations in ${}^{208}\text{Pb}$ [18], in the present case of ${}^{120}\text{Sn}$ it is consistent at least with the selected Skyrme parameter sets. On the other hand, the performance of the present prescription applied to the σ_R data is not good. Therefore we suspect that the σ_R data contain some error.

Next we examine ${}^{116,124}\text{Sn}$. Many data extracted from various methods, which are presented in Fig.4 of Ref. [21], are available in addition to the σ_R data of present interest. Our results are shown in Fig. 4 and Table III. That of ${}^{124}\text{Sn}$ looks consistent with other experimental and theoretical results, but in the ${}^{116}\text{Sn}$ case R_{skin} extracted from σ_R is evidently too large as in the ${}^{120}\text{Sn}$ case above.

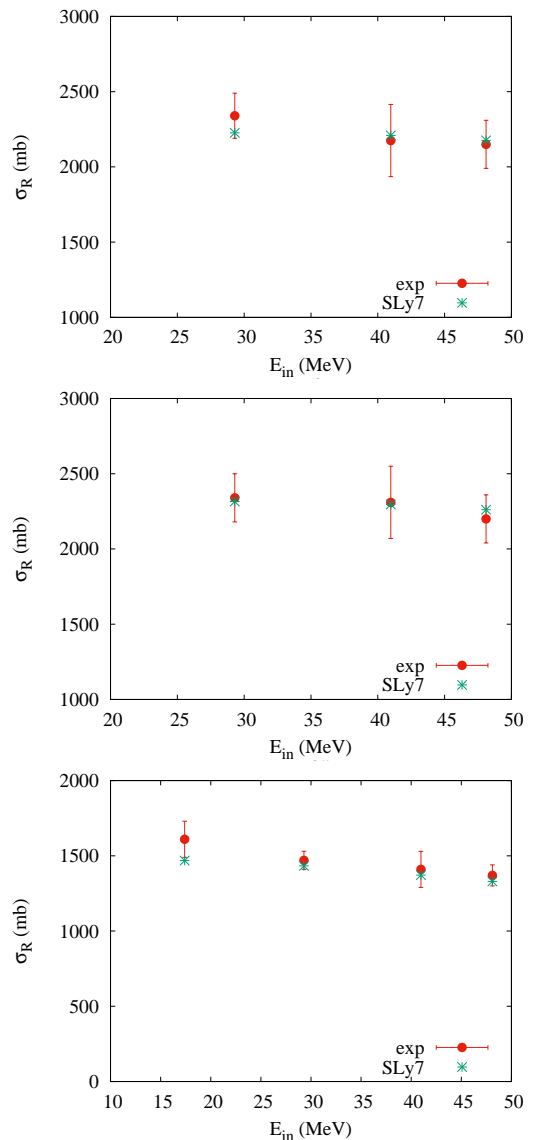


FIG. 4. Three panels from the top to the bottom show E_{in} dependence of reaction cross sections σ_R for ${}^4\text{He} + {}^{116,124}\text{Sn}$, and ${}^{40}\text{Ca}$ scattering, respectively. Asterisks show the results of SLy7-HFB. The data are taken from Ref. [16].

C. ${}^{40}\text{Ca}$

As the last example, we take ${}^{40}\text{Ca}$ in order to see whether the present method is applicable also to the case with $R_{skin} \lesssim 0$. ${}^{48}\text{Ca}$ will be studied separately elsewhere. The results are shown in Fig. 4 and Table III. In Table III, our result is compared with that deduced from the recent proton elastic scattering [25]. These indicate that the present method works well also for the $R_{skin} \lesssim 0$ case, at the same time, indicate that the mean-field parameters of the neutron sector is more reliable than in heavier cases.

TABLE III. Various radii of $^{116,124}\text{Sn}$, and ^{40}Ca , given in fm. Column 1, 4, and 7 are the results of the direct calculations with the Skyrme-HFB. Column 2, 5, and 8 are those of the same renormalization procedure applied to the data [16] with $R_p = 4.554, 4.606,$ and 3.378 fm, determined from the charge density data [22]. Column 3, 6, and 9 are taken from Refs. [23, 25].

	^{116}Sn			^{124}Sn			^{40}Ca		
	SLy7	^4He	Krasznahorkay	SLy7	^4He	Krasznahorkay	SLy7	^4He	Zenihiro
R_n	4.654	4.796 ± 0.140		4.779	4.785 ± 0.142		3.359	3.343 ± 0.075	$3.375^{+0.022}_{-0.023}$
R_p	4.565	4.554		4.623	4.606		3.406	3.378	3.385
R_{skin}	0.089	0.242 ± 0.140	0.12 ± 0.06	0.155	0.180 ± 0.142	0.19 ± 0.07	-0.043	-0.035 ± 0.075	$-0.010^{+0.022}_{-0.024}$
R_m	4.616	4.693 ± 0.140		4.717	4.714 ± 0.142		3.381	3.361 ± 0.075	

IV. SUMMARY

Based on the studies of reaction cross sections that confirm the double folding model with the Kyushu chiral g -matrix at each E_{in} and the Gogny and Skyrme HFB, we examined to deduce the neutron skin thicknesses of ^{208}Pb , $^{116,120,124}\text{Sn}$, and ^{40}Ca . First we found that the present model gives 3.4 % smaller cross sections for $^4\text{He} + ^{208}\text{Pb}$, similarly to 3 % in the single folding case of $p + ^{208}\text{Pb}$ in a preceding work. We attributed the origin of these deviations to less-confirmed mean-field parameters for neutrons in heavy nuclei, and renormalized the HFB densities. Then the nuclear matter radii deduced from cross sections lead to skin thicknesses by confronting precision proton radii. The result is consistent with that of PREX II. Then we applied the method to lighter nuclides. Among stable Sn isotopes, for which the σ_R data show rather large error, this method leads to thicker skins in $^{116,120}\text{Sn}$. This indicates that other observables should also be examined. For ^{40}Ca in which mean-field parameters are thought to be relatively well determined and $R_{\text{skin}} \lesssim 0$, this method works well. We summarize our numerical results for the five nuclides in Fig. 5 as a function of the separation energy difference.

Using the fitted relation between the skin thickness of ^{208}Pb and the slope parameter of symmetry energy, $R_{\text{skin}}^{208} = 0.101 + 0.00147L$ [26], our result $R_{\text{skin}}^{208} = 0.416 \pm 0.146$ fm and R_{skin}^{208} (PREX II) = 0.283 ± 0.071 fm lead to $L = 115 - 313.6$ MeV and $L = 75.5 - 172.1$ MeV, respectively. These

values support stiffer EoSs and exclude APR ($L \approx 40$ MeV). This is the point we found out through the present study in relation to the symmetry energy.

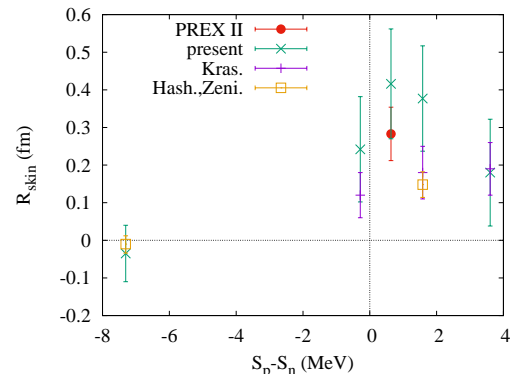


FIG. 5. Skin thicknesses deduced in the present and other works are summarized as a function of the difference between the proton and neutron separation energies: -7.31, -0.28, 0.64, 1.58, and 3.60 MeV for ^{40}Ca , ^{116}Sn , ^{208}Pb , ^{120}Sn , and ^{124}Sn , respectively. The data are taken from Refs. [2, 23–25].

ACKNOWLEDGMENTS

We would like to thank Dr. Toyokawa for providing his code.

-
- [1] C. J. Horowitz, S. J. Pollock, P. A. Souder, and R. Michaels, Phys. Rev. C **63**, 025501 (2001).
 - [2] D. Adhikari et al. (PREX), Phys. Rev. Lett. **126**, 172502 (2021), arXiv:2102.10767 [nucl-ex].
 - [3] A. Akmal, V. R. Pandharipande, and D. G. Ravenhall, Phys. Rev. C **58**, 1804 (1998), arXiv:nucl-th/9804027.
 - [4] B.-A. Li, A. Ramos, G. Verde, and I. Vidana, Eur. Phys. J. A **50**, 9 (2014).
 - [5] M. Toyokawa, M. Yahiro, T. Matsumoto, and M. Kohno, PTEP **2018**, 023D03 (2018), arXiv:1712.07033 [nucl-th].
 - [6] M. Kohno, Phys. Rev. C **88**, 064005 (2013).
 - [7] <https://sites.google.com/view/kyushu-nucl-th/misc/parameter-sets-of-kyushu-chiral-g-matrix>.
 - [8] H. de Vries, C. W. de Jager, and C. de Vries, At. Data Nucl. Data Tables **36**, 495 (1987).
 - [9] S. Tagami, M. Tanaka, M. Takechi, M. Fukuda, and M. Yahiro, Phys. Rev. C **101**, 014620 (2020), arXiv:1911.05417 [nucl-th].
 - [10] S. Tagami, T. Wakasa, J. Matsui, M. Yahiro, and M. Takechi, Phys. Rev. C **104**, 024606 (2021), arXiv:2010.02450 [nucl-th].
 - [11] N. Schunck et al., Comput. Phys. Commun. **216**, 145 (2017), arXiv:1612.05314 [nucl-th].

- [12] E. Chabanat, P. Bonche, P. Haensel, J. Meyer, and R. Schaeffer, Nucl. Phys. A **635**, 231 (1998), [Erratum: Nucl.Phys.A 643, 441–441 (1998)].
- [13] K. Minomo, K. Ogata, M. Kohno, Y. R. Shimizu, and M. Yahiro, J. Phys. G **37**, 085011 (2010), arXiv:0911.1184 [nucl-th].
- [14] K. Egashira, K. Minomo, M. Toyokawa, T. Matsumoto, and M. Yahiro, Phys. Rev. C **89**, 064611 (2014).
- [15] A. B. Jones and B. A. Brown, Phys. Rev. C **90**, 067304 (2014).
- [16] A. Ingemarsson et al., Nucl. Phys. A **676**, 3 (2000).
- [17] M. C. Atkinson, M. H. Mahzoon, M. A. Keim, B. A. Bordelon, C. D. Pruitt, R. J. Charity, and W. H. Dickhoff, Phys. Rev. C **101**, 044303 (2020).
- [18] J. Piekarewicz, “Implications of prex-2 on the electric dipole polarizability of neutron rich nuclei,” (2021), arXiv:2105.13452 [nucl-th].
- [19] A. Tamii, I. Poltoratska, P. von Neumann-Cosel, Y. Fujita, T. Adachi, C. A. Bertulani, J. Carter, et al., Phys. Rev. Lett. **107**, 062502 (2011).
- [20] P.-G. Reinhard and W. Nazarewicz, Phys. Rev. C **81**, 051303 (2010).
- [21] P. Sarriguren, M. K. Gaidarov, E. M. d. Guerra, and A. N. Antonov, Phys. Rev. C **76**, 044322 (2007).
- [22] I. Angeli and K. Marinova, At. Data Nucl. Data Tables **99**, 69 (2013).
- [23] A. Krasznahorkay et al., Phys. Rev. Lett. **82**, 3216 (1999).
- [24] T. Hashimoto et al., Phys. Rev. C **92**, 031305 (2015), arXiv:1503.08321 [nucl-ex].
- [25] J. Zenihiro, H. Sakaguchi, S. Terashima, T. Uesaka, G. Hagen, M. Itoh, T. Murakami, Y. Nakatsugawa, T. Ohnishi, H. Sagawa, H. Takeda, M. Uchida, H. P. Yoshida, S. Yoshida, and M. Yosoi, “Direct determination of the neutron skin thicknesses in $^{40,48}\text{Ca}$ from proton elastic scattering at $e_p = 295$ mev,” (2018), arXiv:1810.11796 [nucl-ex].
- [26] X. Roca-Maza, M. Centelles, X. Vinas, and M. Warda, Phys. Rev. Lett. **106**, 252501 (2011), arXiv:1103.1762 [nucl-th].